Methylmercury complexes: Selection of thermodynamic properties and application to the modelling of a column experiment

Philippe Blanc, André Burnol, Nicolas C.M. Marty, Jennifer Hellal, Valérie Guérin, Valérie Laperche

METHYLMERCURY COMPLEXES: SELECTION OF THERMODYNAMIC PROPERTIES AND APPLICATION TO THE MODELLING OF A COLUMN EXPERIMENT

P. Blanc, A. Burnol, N. Marty, J. Hellal, V. Guérin, V. Laperche*

BRGM, 3 Avenue Claude Guillemin, 45060 Orléans Cedex 2, France
* Corresponding author: p.blanc@brgm.fr

Abstract

Complexation with methyl groups produces the most toxic form of mercury, especially because of its capacity to bioconcentrate in living tissues. Understanding and integrating methylation and demethylation processes is of the utmost interest in providing geochemical models relevant for environmental assessment. In a first step, we investigated methylation at equilibrium, by selecting the thermodynamic properties of different complexes that form in the chemical system Hg-SO_3-S-Cl-C-H_2O. The selection included temperature dependencies of the equilibrium constants when available. We also considered adsorption and desorption reactions of both methylated and non-methylated mercury onto mineral surfaces. Then we assessed the kinetics of methylation by comparing a dedicated column experiment with the results of a geochemical model, including testing different methylation and demethylation kinetic rate laws. The column system was a simple medium: silicic sand and iron hydroxides spiked with a mercury nitrate solution. The modelling of methylmercury production with two different rate laws from the literature is bracketing the experimental results. Dissolved mercury, iron and sulfate concentrations were also correctly reproduced. The internal evolution of the column was also correctly modeled, including the precipitation of mackinawite (FeS) and the evolution of dissolved iron. The results validate the conceptual model and underline the capacity of geochemical models to reproduce some processes driven by bacterial activity.

Keywords: Methylmercury, reactive transport, percolation, sulfate reduction

Introduction

Mercury (Hg) is among the most toxic elements, and has many natural sources. Human activity, especially mining and the burning of coal, has increased the mobilization of mercury into the environment. For about 200 years, anthropogenic emissions have been greater than natural emissions (UNEP, 2013). Mercury occurs in various chemical forms. Most atmospheric Hg is gaseous elemental mercury (Hg^0). In surface water and soils it occurs as elemental mercury (droplets of liquid mercury) and as Hg(II) complexes (Kim et al., 2003). Hg-containing minerals, such as cinnabar and metacinnabar (two polymorphs of HgS) and montroydite (HgO), can control its solubility (Kim et al., 2003). Much human exposure to mercury is through the consumption of fish and other marine foods, since mercury is mainly introduced into the food chain as methylmercury (MeHg). In soils, the presence of MeHg results from a balance between different competing processes (Skyllberg, 2012): methylation and demethylation (Cossa et al., 2014) reactions, formation of aqueous complexes and gaseous species and adsorption/desorption reactions onto inorganic and organic substrates. The balance between those different mechanisms determines bioaccumulation and MeHg transportation.

Researchers have begun to use geochemical modelling to assess the fate of mercury in the environment. Bessinger et al. (2012) have proposed a comprehensive model to reproduce mercury and arsenic speciation in sediment caps and how it changes over time, including MeHg. Leterme et al. (2014) also developed geochemical modelling of a conceptual soil, to assess the relative proportion of mercury release in the atmosphere or transported through the soil column or trapped, either onto mineral surfaces or as minerals precipitated along the profile.

Leterme et al. (2014) explained that in spite of being an important tool, geochemical modelling suffers from the lack of well characterized sites. Actually, the counterpart of being

able to reproduce detailed reactive mechanisms is that those models may require an important input dataset, including site-specific parameters. Even if determined, the values may suffer from variability and heterogeneities. As an alternative, we propose building a model to reproduce the results of a less complex column experiment. The model itself would include all the complexity governing MeHg fate, including methylation/demethylation reactions, the formation of aqueous complexes and gaseous species and surface complexation reactions. Johannesson and Neumann (2013) conducted a comprehensive set of measurements in groundwater along a 13 km flowpath located within a confined aquifer in southeastern Texas, USA. Their biogeochemical model was able to highlight the main mechanisms (mineral dissolution and sorption onto oxide surfaces) responsible for the speciation of total Hg.

The aim of this study is to test geochemical modelling in a more controlled context like the column experiment performed by Hellal et al. (2015). The geochemical calculations on Hg fate can then be somehow constrained or compared with respect to those experimental results. In addition, taking advantage of the analyses performed by Hellal et al. (2015), the calculations are especially focused on methylmercury fate (methylation/demethylation and transportation), allowing testing of the methylation/demethylation rates available to date in the literature. Before comparing the calculations with the experimental results, we include a critical selection for MeHg complexes, consistent with the database built up by Leterme et al. (2014) for Hg-bearing species. The selection extended to surface complexation reactions and methylation/demethylation rates, following the review and case study proposed by Bessinger et al. (2012) and Cossa et al. (2014).

1. Selection of thermodynamic properties for methylmercury aqueous complexes

Methylmercury is a strongly toxic complex that accumulates in the muscles and various living tissues of living organisms. After Thomassin and Touze (2003), the methylation of mercury is favored in anoxic environments by the presence of sulfate-reducing bacteria and of sulfur. Generally speaking, the methylation reaction proceeds this way:

$$\begin{aligned} Hg^{++} + CH_{4,aq} &\xrightarrow{\text{Bacteria}} CH_3Hg^+ + H^+ && \text{Mono-MethylMercury (MMHg)} \\ CH_3Hg^+ + CH_{4,aq} &\xrightarrow{\text{Bacteria}} (CH_3)_2Hg + H^+ && \text{Di-MethylMercury (DMHg)} \end{aligned} \quad (1)$$

Dimethyl products are found as both aqueous complexes (in basic solutions) and in gaseous form. Methylation of mercury is reversible. We selected MeHg species using thermodynamic data processed according to guidelines describes by Blanc et al. (2012) and consistent with the previous selection by Leterme et al. (2014). The thermodynamic parameters associated with complexation reactions have been collected and discussed from Erni (1977), Alderighi et al. (2003), Loux (2007) and Skyllberg (2012), for various chemical systems, at 25°C. Loux (2007) are especially important, resulting from an extrapolation to infinite dilution of large experiment datasets. Alderighi et al. (2003) have measured, by calorimetry, the heat exchanged during various complexation reactions involving methylmercury. From these measurements, we were able to calculate the entropy of complexes, which are reported in Table 1. Actually, they provided ΔS_r for reactions involving CH_3Hg^+ as primary specie. In order to use these measurements, we have considered the reaction:

$$Hg^{++} + CH_{4,aq} \longrightarrow CH_3Hg^+ + H^+ \quad (2)$$

It was converted into an isocoulombic equilibrium using Ca++ and Ca(OH)+ species:

$$Hg^{++} + CH_{4,aq} + CaOH^{+} \longrightarrow CH_3Hg^{+} + Ca^{++} + H_2O \quad (3)$$

The third law entropy was calculated considering the one term approximation method from Gu et al. (1994) and entropies from the Thermoddem database (Blanc et al., 2012). The result allows obtaining the third law entropies from Alderighi et al. (2003) measurements. The whole results are reported in Table 1. In addition to the aqueous complexes we have included a gas phase, $Hg(CH_3)_{2,g}$ which represents an extreme stage of the methylation process (Thomassin and Touze, 2003).

Table 1 – Selection for thermodynamic properties of MeHg-bearing species

Specie	**Equilibrium**	**$Log_{10}K$ (298.15 K)**	**S° (J/mol.K)**	**References**
CH_3^-	$CH_{4,aq} = CH_3^- + H^+$	-46.00		(1)
CH_3Hg^+	$CH_{4,aq} + Hg^{++} = CH_3Hg^+ + H^+$	3.00	65.91	(1), this work
CH_3HgCl	$CH_3Hg^+ + Cl^- = CH_3HgCl$	5.45	142.91	(2), (3)
CH_3HgOH	$CH_3Hg^+ + H_2O = CH_3HgOH + H^+$	-4.53	110.71	(2), (3)
CH_3HgS^-	$CH_3Hg^+ + HS^- = CH_3HgS^- + H^+$	4.00		(2)
CH_3HgSH	$CH_3Hg^+ + HS^- = CH_3HgSH$	14.50		(2)
$(CH_3)_2Hg$	$2CH_3Hg^+ = (CH_3)_2Hg + Hg^{++}$	13.00		(1)
$CH_3HgCO_3^-$	$CH_3Hg^+ + HCO_3^- = CH_3HgCO_3^- + H^+$	-4.23		(2)
CH_3HgHCO_3	$CH_3Hg^+ + HCO_3^- = CH_3HgHCO_3$	2.60		(2)
$CH_3HgSO_4^-$	$CH_3Hg^+ + SO_4^{--} = CH_3HgSO_4^-$	2.64		(2)
$(CH_3Hg)_2OH^+$	$2CH_3Hg^+ + H_2O = (CH_3Hg)_2OH^+ + H^+$	-2.15	167.62	(2), (3)
$(CH_3Hg)_2S$[a]	$CH_3Hg^+ + CH_3HgS^- = (CH_3Hg)_2S$	20.32		(2)
$Hg(CH_3)_{2,g}$	$Hg^{++} + 2CH_{4,aq} = Hg(CH_3)_{2,g} + 2H^+$	8.82	306.00	(4)

(1) Erni (1977); (2) Loux (2007); (3) recalculated using reaction entropy from Alderighi et al. (2003); (4) Wagman et al. (1982)

a. Not selected (see text)

For the selection, we followed the approach promoted by Stumm and Morgan (1996) where the methyl group is represented by the CH_3^- anion. This formally identifies the methylated complexes and easily separates the inorganic and organic chemical system when required. The selection was integrated in the Thermoddem database (Blanc et al., 2012) in order to

use it with geochemical codes GWB (Bethke, 2004) and PhreeqC (Parkhurst and Appelo, 1999).

A first test of the database consisted in calculating the production of methyl complexes which would arise from the speciation model detailed in Table 1. After Leterme and Jacques (2012), the amount of MeHg in waters in contact with soil systems is usually close to 2%. A speciation calculation is conducted, using PhreeqC-2 with the above database and considering a solution with [NaCl] = with 10^{-3} M and [Hg] = 10^{-9} M. This amount was reached applying two different corrections:

- by modifying reaction (2) equilibrium constant from $\log_{10}K = 3$ to 2.5 when reactions from Table 1 a written with $CH_{4,aq}$ as primary specie
- or by modifying $CH_{4,aq} = CH_3^- + H^+$ equilibrium constant from $\log_{10}K = -46$ to -52.5 when reactions from Table 1 a written with CH_3^- as primary specie.

Actually, we did not expect the relation between organic and inorganic carbon to be driven by thermodynamic equilibrium. The correction considered in the first test is still of small extent, especially because the value originally given by Erni (1977) was calculated and not measured and the uncertainty can be larger in that case. In addition, the fact that the results obtained for MeHg speciation may depend on the way the database is written is to be underline. For the rest of the calculations, we no longer consider the equilibrium between organic and inorganic reduced carbon. However it is important to note that when the database uses $CH_{4,aq}$ or CH_3^- complexes as primary specie for the methylation reactions, this allows considering also the methylation for other metals like Sn or Pb (Stumm and Morgan, 1996), jointly with Hg methylation. The database in Table 1 was also tested using activity diagrams of which examples are displayed in Figure 1

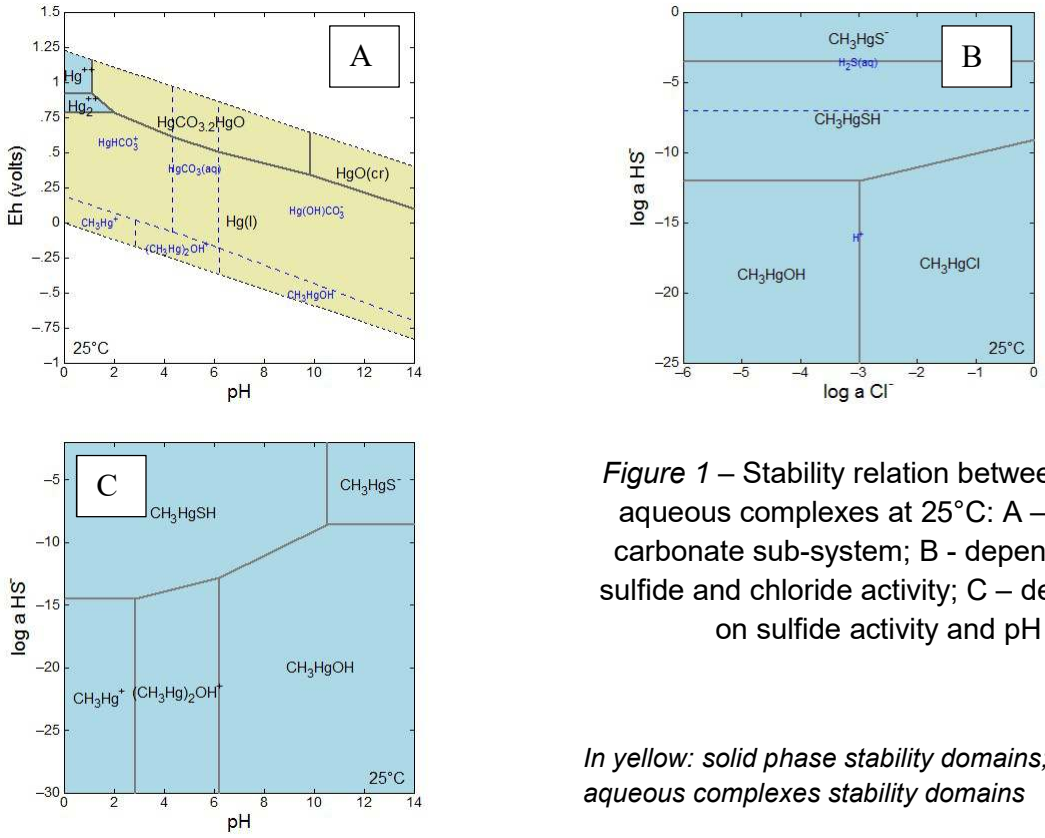

Figure 1 – Stability relation between MeHg aqueous complexes at 25°C: A – for the carbonate sub-system; B - depending on sulfide and chloride activity; C – depending on sulfide activity and pH

In yellow: solid phase stability domains; in blue: aqueous complexes stability domains

The carbonate stability domains (Figure 1.A) are in agreement with Powell et al. (2005) calculations. As for methylmercury species, they are dominated by CH_3Hg^+, $(CH_3Hg)_2OH^+$ and CH_3HgOH complexes and located in the reduced part of the predominance diagram. The equilibrium with dissolved carbonate species strongly reduces the methylmercury stability domain. Since most of the contaminated water contains 1% of total mercury as MeHg, this would imply kinetic control of MeHg speciation. Figures 1.B and 1.C display a transition between sulfide and hydroxylated species for a total sulfide concentration close to 10^{-12} mol/L, whereas Boszke et al. (2002) proposed 10^{-11} mol/L. On the other hand the transition between chlorinated and hydroxylated methyl complexes occurs according to Boszke et al.'s calculation at pH = 7 (for a chloride concentration of about 10^{-3} mol/L). Previous results could only be obtained only by removing the $(CH_3Hg)_2S$ complex which displayed an exaggerated stability, covering most of the area in figures 1.B and 1.C.

2. Column experiment (Hellal et al., 2015)

The database set up previously is now tested by modeling the MeHg rate obtained experimentally by Hellal et al. (2015) in a companion. To our knowledge, such comparison is rather unique for Hg methylation, up to now.

Only a brief description is given here and the reader referred to Hellal et al. (2015) for additional details. The experiment design is reported in Figure 2. The lower half the column is filled with sterile sand and the upper half with a sterile mixture of sand and iron oxides, initially enriched with Hg(+2). The column is inoculated with a bacterial consortium and the inflowing solution is supplemented with magnesium sulfate and sodium lactate to enhance the growth and activity of sulfate-reducing bacteria (SRB). The water flow is ascendant. Five septa set regularly along the columns enable water sampling from the different layers of the column without perturbing water flow or in situ experimental conditions. After an abiotic rinsing period, the system is inoculated with a bacterial consortium, and physical, chemical and microbial parameters are monitored in time and space, up to 143 days.

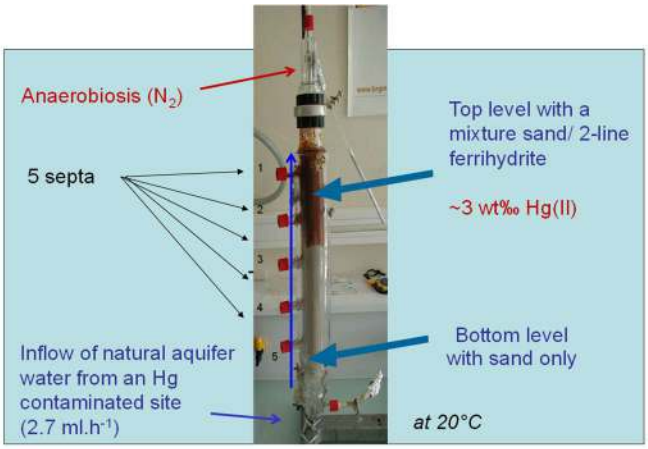

Analyses:
- pH, Eh
- Dissolved Fe, Fe(II), S(6), S(-2)
- Hg, MeHg
- Solid products (Raman spectroscopy)
- Bacterial diversity (DGGE, FISH)

- **Percolating water (mmol.L^{-1}):** pH 7.22, pe 2.28, [Ca] 1.41, [Cl] 0.42, [Na] 0.30, [S] 0.75, [Lactate] 0.01, [Fe] 1.80.10^{-7}, [Hg] 1.6.10^{-9}
- **Solid matrix:** 0-15 cm sand ; 15-30 cm sand + Ferrihydrite 2L (5.7 %)
- Percolating water inoculated with SRB and FRB
- Percolating for 143 days

Figure 2 – Experimental design developed by Hellal et al. (2015)

3. Model development

A specific reactive transport model was developed to reproduce the experimental conditions. Methylation is described in the model following a suite of chemical reactions described in Figure 3, where MeHg formation arises from a rather complex process including different steps:

- a first step corresponds to the reduction of Fe(+3) from the dissolution of ferrihydrite. It is reproduced using the model developed by Poulton (2003)
- meanwhile, sulfate undergoes a reduction induced by the activity and growth of SRB bacteria. The reduction is modeled using a first order rate law which rate constant is extracted from Bharati and Kumar (2012) experiment (Table 2)
- both Fe(+2) and S(-2) are consumed to precipitate mackinawite ($FeS_{,cr}$)

- cobaltihexamine ($CoB\text{-}CH_3$) complexes with mackinawite surfaces, the methyl group CH_3^- is released and combines in solution with dissolved mercury Hg^{++} to form eventually the methylmercury complex CH_3Hg^+. Two rate laws were tested, a first order proposed by Bessinger et al. (2012) and a second law based on the work by Heyes et al. (2006) (Table 2) and which rate corresponds to a balance between both methylation and demethylation rates.

The possible formation of complexes at the ferrihydrite surface is implemented, using capacity of ferrihydrite, using the Dzombak and Morel (1990) model and database. Numerical modelling uses PhreeqC-2 code (Parkhurst and Appelo, 1999) and the Thermoddem database (Blanc et al., 2012). The conceptual model is based on 1D-cartesian geometry, as displayed in Figure 4. A tracer test has been successfully simulated to verify the hydrodynamic set of parameters used.

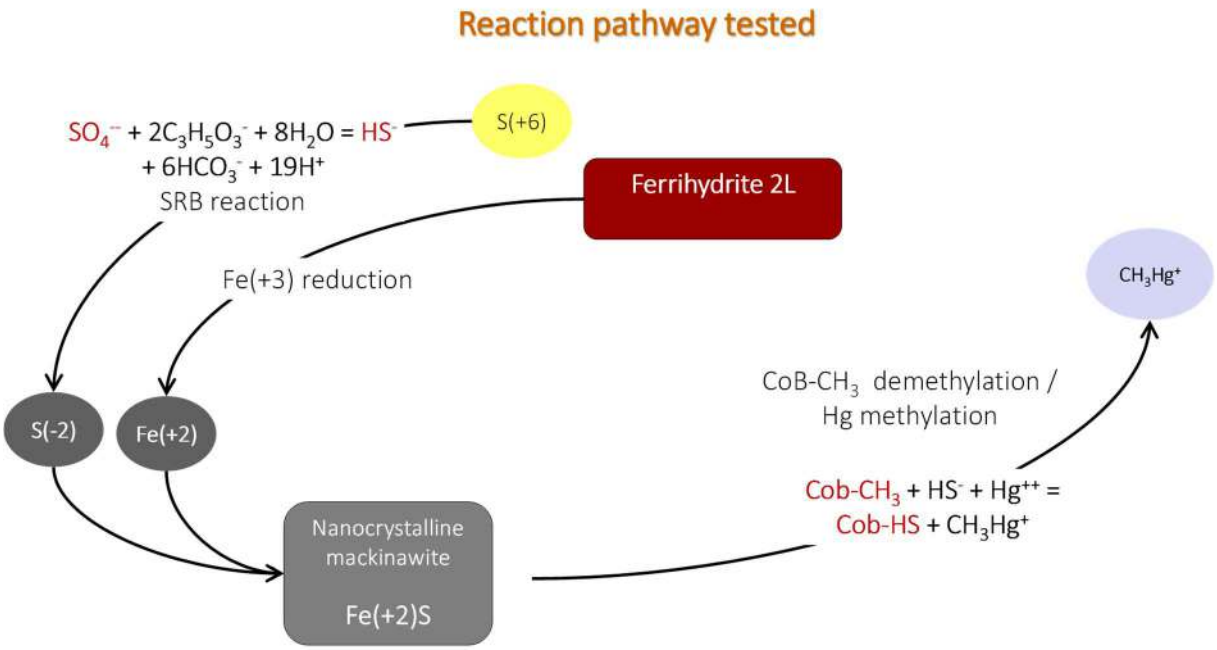

Figure 3 – Main reactions involved

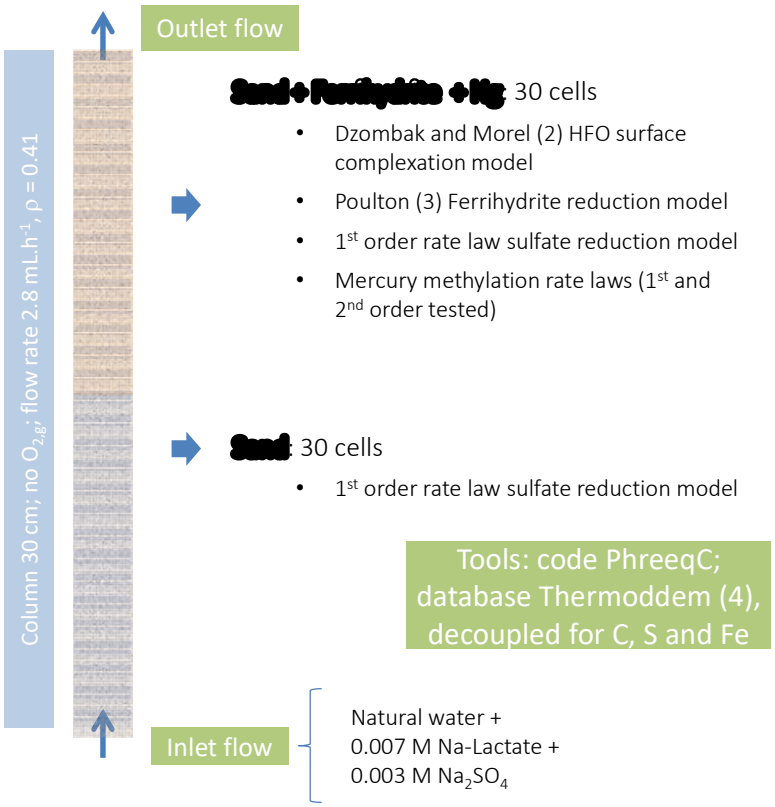

Figure 4 – Conceptual model

Table 2 – Main parameters for reactive transport modeling

Chemical system			
Minerals			
Ferrihydrite	$Fe(OH)_3 + 3H^+ = Fe^{+++} + 3H_2O$	$Log_{10}K° = 3.40$	Blanc et al. (2012)
Mackinawite	$FeS + H^+ = Fe^{++} + HS^-$	$Log_{10}K° = -3.54$	Blanc et al. (2012)
Schwertmannite	$Fe_8O_8(OH)_6SO_4{:}8H_2O + 22H^+ = 8Fe^{+++} + SO_4^{--} + 22H_2O$	$Log_{10}K° = 8.95$	Blanc et al. (2012)
Calcite	$CaCO_3 + H^+ = HCO_3^- + Ca^{++}$	$Log_{10}K° = 1.85$	Blanc et al. (2012)
Aqueous species			
Thermoddem database, decoupled	C decoupled into C(+4) and C(-4) S decoupled into S(+6) and S(-2) Fe decoupled into Fe(+2) and Fe(+3)	Percolating solution given Figure 2	
Surface complexation			
Ferrihydrite surface	$>Fe^sOH + X^z = >FeOX^{(z-1)} + (z-1)H^+$ $>Fe^wOH + X^z = >FeOX^{(z-1)} + (z-1)H^+$	X^z= Fe^{++}, Hg^{++}, Ca^{++}, SO_4^{--}, H^+	Dzombak and Morel (1990)
Mackinawite surface	$>FeS + CH_3Hg^+ = >FeS-CH_3Hg^+$	$Log_{10}K° = 4.5$	This study
Kinetic transformations			
Sulfate reduction	$SO_4^{--} + 2C_3H_5O_3^- + 8H_2O = HS^- + 6HCO_3^- + 19H^+$	$k_{sr} = 6\ 10^{-7}\ s^{-1}$	Extracted from Bharati and Kumar (2012)
MeHg formation	Model1: $k_1\ (s^{-1}) = [Hg(HS)_2]\cdot k_{sr}\cdot 4.2\ 10^5$ Model2: Cob-CH_3 + HS^- + Hg^{++} = Cob-HS + CH_3Hg^+	$k_2 = 1.3\ 10^{-7}\ s^{-1}$	Bessinger et al. (2012) Heyes et al. (2006)
Fe reduction	$k_{fe}\ (s^{-1}) = 0.92\ 10^{-6}\cdot[\text{Ferrihydrite}]\cdot[S(-2)]^{0.5}$		Poulton (2003)
Physical parameters			
Porosity = 0.41	Extracted from a preliminary tracing test	0.41	This study
Inlet solution flow		2.8 mL/h	Hellal et al. (2015)

4. Results and discussion

The results were first verified at the column breakthrough point (Figure 5) and along the column (Figure 6) for the longest reaction time (143 days). The reduction of sulfates was correctly reproduced, globally. In that regard, Bharati and Kumar (2012) experiment was selected because they were performing sulfate reduction by using lactate as substrate and carbon source, as in our case. However, sulfate reduction appears somewhat underestimated by the model, especially concerning sulfide production. The redox conditions in the column (and departure to equilibrium conditions) could be questioned in that regard. Dissolved Fe(+2) at the outlet was quite correctly predicted and calculations corresponding to the concentrations measured in the different septa even matched the abrupt increase observed in the ferrihydrite-loaded part of the column. Such increase happens during a period when calcite precipitates. It also corresponds to the precipitation of Mackinawite, observed in the experiments by Hellal et al. (2015), using Raman spectroscopy. From the reaction displayed in Table 2, mackinawite precipitation happens to consumes protons which increases pH and can lead induce the precipitation of carbonates.

For dissolved mercury (Figure 5), the total concentrations were correctly predicted. Methylmercury concentrations analyzed were somewhat bracketed by the calculation performed with the model proposed by Bessinger et al. (2012) and Heyes et al. (2006) (Model 1 and Model 2 in Figure 5, and Table 2 respectively). The lowest concentrations found using Heyes et al (2006) methylation rate law may possibly be explained because the first order rate constant reported in Table 2 represent a balance between both methylation and demethylation rates. Actually the global methylation budget usually arises from the competition between both mechanisms.

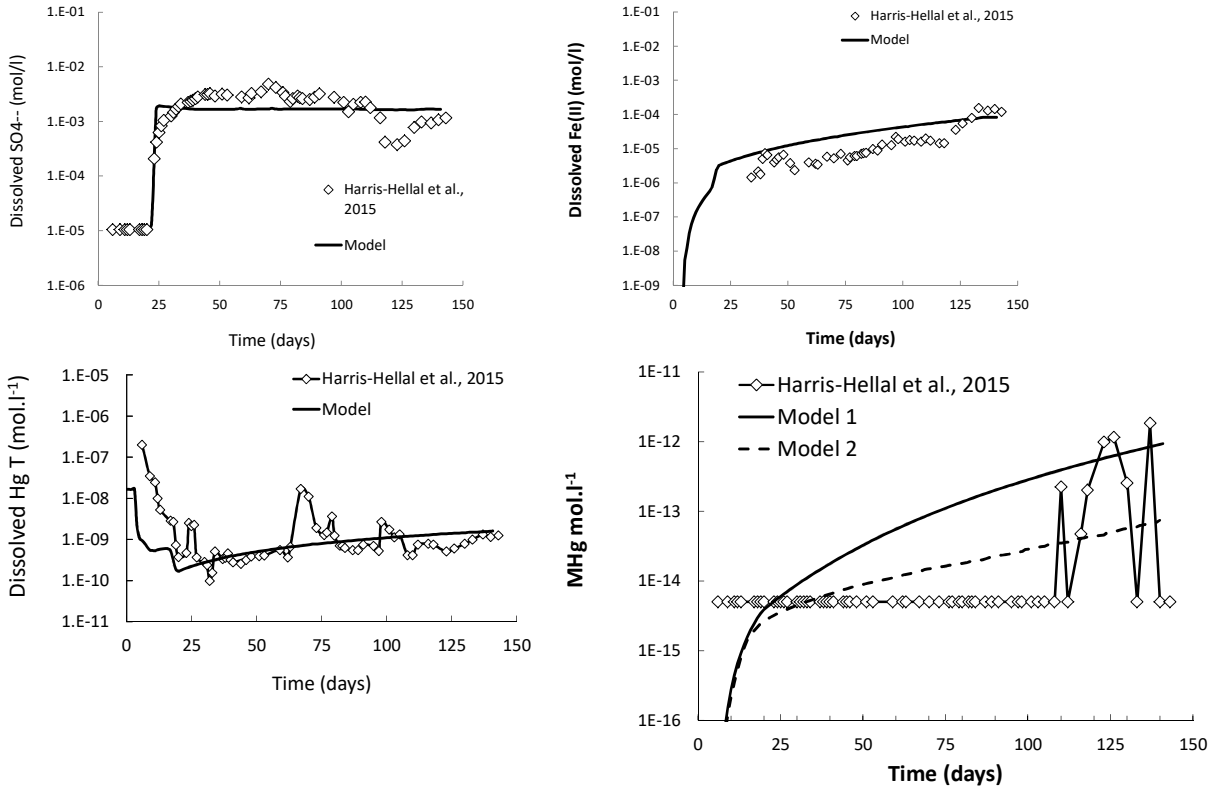

312 *Figure 5* – Concentration in dissolved elements analysed at the outlet of the column

313
314

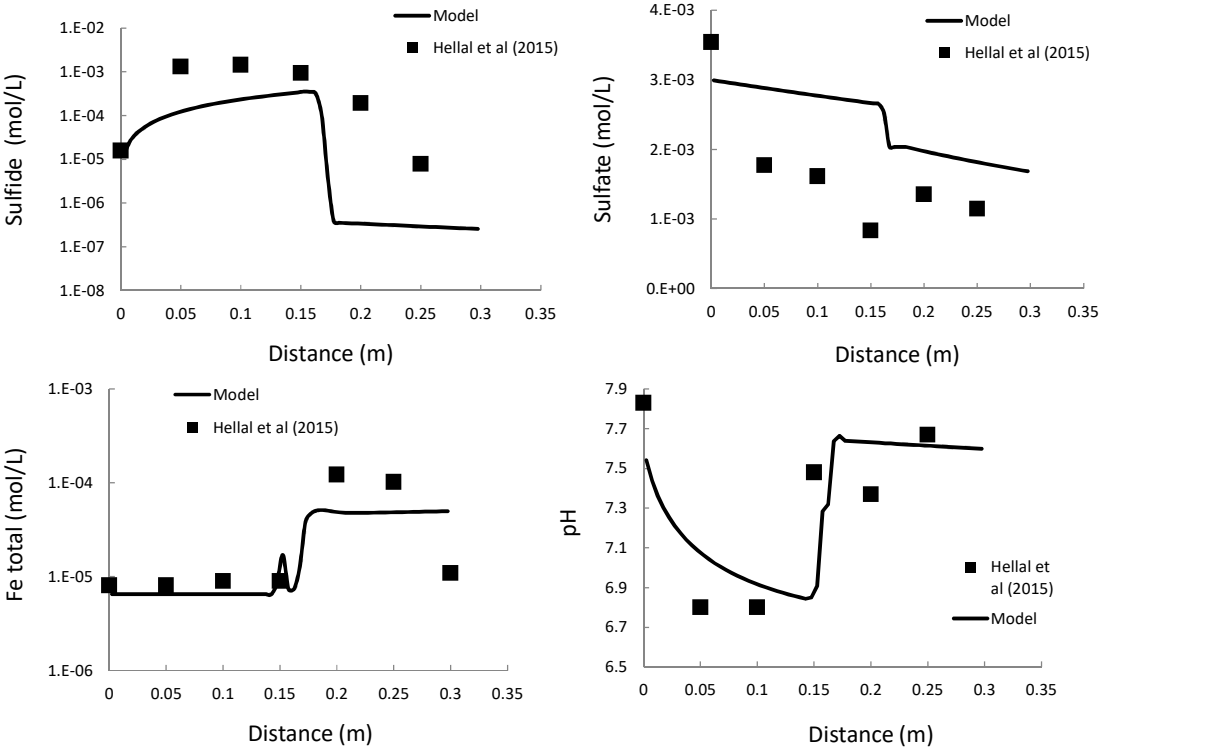

315
316
317

318 *Figure 6* – Concentration in dissolved elements in the length of the column, after 143 days. 0
319 (m) corresponds to the inlet solution

Conclusion

The results obtained here are in line with previous works from Bessinger et al. (2012) and Leterme et al. (2014). However, it displays a rare comparison between experiment and reactive transport modelling results. It confirms the rate obtained by previous authors concerning the mercury methylation process and it brings a confirmation to the reaction pathways first proposed by Hellal et al. (2015) to explain their evolutions. The selection of thermodynamic properties for MeHg complexes gave the opportunity to test different writing for the MeHg database. The testing favored the discarding of the dimethyl complex $(CH_3)_2Hg$ from the thermodynamic dataset. In addition, it enhances possible connections between inorganic and organic dissolved carbon forms, from the point of view of methylation processes. Such relations do probably not involve equilibrium reaction. There is a strong need for additional experiment data to test such hypotheses, including measurements that does not seems to be related, at first sight, like dissolved CH_4 concentrations, for instance.

ACKNOWLEDGEMENTS

Financial support from the French Geological Survey (BRGM, Geomer Project) and from the EU through the Snowman IMAHg project is gratefully acknowledged. The authors would like to thank for BA Bessinger for his kind help.

References

Alderighi L, Gans P, Midollini S, Vacca A. Co-ordination chemistry of the methylmercury(II) ion in aqueous solution: a thermodynamic investigation. Inorganica Chimica Acta 2003; 356: 8-18.

Bessinger BA, Vlassopoulos D, Serrano S, O'Day PA. Reactive Transport Modeling of Subaqueous Sediment Caps and Implications for the Long-Term Fate of Arsenic, Mercury, and Methylmercury. Aquatic Geochemistry 2012; 18: 297-326.

Bethke C. GWB Reference Manual: RockWare Incorporated, 2004.

Bharati B, Kumar GP. A study on efficiency of five different carbon sources on sulfate reduction. Journal of Environmental Research And Development Vol 2012; 7.

Blanc P, Lassin A, Piantone P, Azaroual M, Jacquemet N, Fabbri A, et al. Thermoddem: A geochemical database focused on low temperature water/rock interactions and waste materials. Applied Geochemistry 2012; 27: 2107-2116.

Boszke L, Glosinska G, Siepak J. Some aspects of speciation of mercury in water environment. Polish Journal of Environmental Studies 2002; 11: 285-298.

Cossa D, Garnier C, Buscail R, Elbaz-Poulichet F, Mikac N, Patel-Sorrentino N, et al. A Michaelis–Menten type equation for describing methylmercury dependence on inorganic mercury in aquatic sediments. Biogeochemistry 2014; 119: 35-43.

Dzombak DA, Morel FM. Surface complexation modeling: hydrous ferric oxide: John Wiley & Sons, 1990.

Erni IW. Relaxationskinetische Untersuchungen von Methylquecksilberübertragungsreaktionen. Chemistry Dept. Ph.D. Swiss Federal Institute of Technology, Zurich,, 1977.

Gu Y, Gammons CH, Bloom MS. A one-term extrapolation method for estimating equilibrium constants of aqueous reactions at elevated temperatures. Geochimica et Cosmochimica Acta 1994; 58: 3545-3560.

374 Hellal J, Guédron S, Huguet L, Schäfer J, Laperche V, Joulian C, et al. Mercury mobilization
375 and speciation linked to bacterial iron oxide and sulfate reduction: A column study to
376 mimic reactive transfer in an anoxic aquifer. Journal of Contaminant Hydrology 2015;
377 180: 56-68.
378 Heyes A, Mason RP, Kim E-H, Sunderland E. Mercury methylation in estuaries: Insights from
379 using measuring rates using stable mercury isotopes. Marine Chemistry 2006; 102:
380 134-147.
381 Johannesson KH, Neumann K. Geochemical cycling of mercury in a deep, confined aquifer:
382 Insights from biogeochemical reactive transport modeling. Geochimica et
383 Cosmochimica Acta 2013; 106: 25-43.
384 Kim CS, Bloom NS, Rytuba JJ, Brown GE. Mercury Speciation by X-ray Absorption Fine
385 Structure Spectroscopy and Sequential Chemical Extractions: A Comparison of
386 Speciation Methods. Environmental Science & Technology 2003; 37: 5102-5108.
387 Leterme B, Blanc P, Jacques D. A reactive transport model for mercury fate in soil-
388 application to different anthropogenic pollution sources. Environmental Science and
389 Pollution Research International 2014.
390 Leterme B, Jacques D. Literature Review: Mercury fate and transport in Soil Systems. SCK-
391 CEN, Boeretang, 2012, pp. 21.
392 Loux NT. An assessment of thermodynamic reaction constants for simulating aqueous
393 environmental monomethylmercury speciation. Chemical Speciation & Bioavailability
394 2007; 19: 183-196.
395 Parkhurst DL, Appelo CaJ. User‘s guide to PHREEQC (Version 2) : a computer program for
396 speciation, batch-reaction, one-dimensional transport, and inverse geochemical
397 calculations. United States Geological Survey, 1999.
398 Poulton SW. Sulfide oxidation and iron dissolution kinetics during the reaction of dissolved
399 sulfide with ferrihydrite. Chemical Geology 2003; 202: 79-94.
400 Powell KJ, Brown PL, Byrne RH, Gajda T, Hefter G, Sjöberg S, et al. Chemical speciation of
401 environmentally significant heavy metals with inorganic ligands. Part 1: The Hg2+–

Cl–, OH–, CO32–, SO42–, and PO43– aqueous systems (IUPAC Technical Report). Pure and Applied Chemistry 2005; 77: 739-800.

Skyllberg U. Chemical Speciation of Mercury in Soil and Sediment. Environmental Chemistry and Toxicology of Mercury. John Wiley & Sons, Inc., 2012, pp. 219-258.

Stumm W, Morgan JJ. Aquatic chemistry: chemical equilibria and rates in natural waters: Wiley, 1996.

Thomassin JF, Touze S. Le mercure et ses composés . Comportement dans les sols, les eaux et les boues de sédiments. Rapport final. , Orleans, 2003, pp. 119.

UNEP. Global Mercury Assessment 2013: Sources, Emissions, Releases and Environmental Transport, 2013, pp. 44.

Wagman DD, Evans WH, Parker VB, Schumm RH, Halow I, Balley SM, et al. NBS Tables of Chemical Thermodynamic Properties: Selected Values for Inorganic and C1 and C2 Organic Substances in SI Units. Journal of Physical and Chemical Reference Data 1982; 11: 1-392.